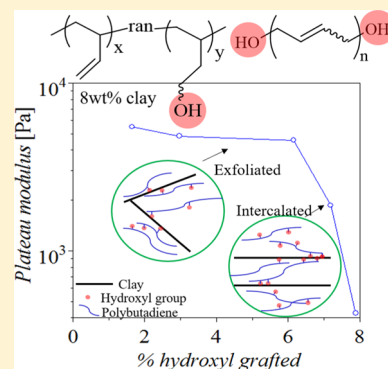


Functionalized Polybutadiene for Clay–Polymer Nanocomposite Fabrication

Vijesh A. Tanna,[†] Joshua S. Enokida,[†] E. Bryan Coughlin,[†] and H. Henning Winter^{*,†,‡}[†]Department of Polymer Science and Engineering and [‡]Department of Chemical Engineering, University of Massachusetts Amherst, Amherst 01003, United States

Supporting Information

ABSTRACT: For polymer nanocomposites with two-dimensional filler materials, intercalation/exfoliation is required to maximize internal connectivity. Previous work has shown that clay exfoliation can be achieved through mild thermal annealing in the presence of a low-molecular-weight, hydroxyl-terminated “telechelic” polybutadiene (tPB) matrix. However, the specific role of the hydroxyl groups, their placement, and polymer mobility in the intercalation/exfoliation process still remains unclear. In this study, these matrix parameters were evaluated by replacing the tPB with randomly functionalized polybutadienes (rPBs) of increasing hydroxyl group densities. The rPB was synthesized by covalently grafting mercaptoethanol to the PB backbone, and its ability to exfoliate organically modified montmorillonite clay was evaluated. While some functional groups are required to exfoliate the clay, it was found that exfoliation proceeds successfully regardless of the number of hydroxyl groups or their location on the PB backbone. Instead, it was found that polymer mobility played a key role in the extent of exfoliation. As the grafting concentration was increased, the rPB molecular mobility decreased because of its higher glass transition temperature (T_g). A detailed analysis of their linear viscoelastic properties was able to decouple the two phenomena, change in mobility and effectiveness of polymer–clay interaction. Nanocomposites using highly grafted polymers showed a decrease in their connectivity because of reduced exfoliation of the clay. This was overcome by introducing a highly grafted and highly mobile rPB with a low T_g (low vinyl content), which successfully exfoliated the clay. The combined results suggest that intercalation can be achieved through favorable polymer–clay interactions, whereas exfoliation can proceed beyond intercalation only when there is enough polymer mobility.



INTRODUCTION

Nanocomposites composed of two-dimensional (2D) nanoparticles dispersed in a polymer matrix are highly desired for applications such as separation membranes, advanced conductive materials, and reinforced composites.^{1–3} The high aspect ratio of the 2D nanoparticles allows for reaching a percolation threshold at relatively low loadings compared to the threshold conditions for spherical particles. Common examples of 2D nanoparticles include clay, graphene, transition metal dichalcogenides, and layered metal oxides. Clay–polymer nanocomposites have been researched extensively, especially to gain insight into the formation of these materials.⁴

The interest in clay–polymer nanocomposites stems from the clay’s ability to increase the internal connectivity of a polymer matrix, which expresses itself through higher modulus values and longer characteristic relaxation times. This increased connectivity was first demonstrated by researchers at Toyota who observed a 3-fold increase in modulus due to clay intercalation.⁵ The origin of connectivity can stem from either polymer–clay interactions or clay–clay interactions, both of which have been reported in the literature.⁴ Polymer–clay interactions have been observed for many polymer composites, such as polyurethane and polycarbonate polymer–clay composites. The enhancement in the material’s mechanical

properties was attributed to hydrogen bonding between the polymer and the clay.^{6,7} In another instance, clay–clay interactions have been reported to result in the formation of a “house of cards” structure in a polypropylene/clay composite.⁸ Such structure formation was attributed to electrostatic interactions between the positively charged edges of the clay particles compared to their negatively charged surfaces.^{9–11} In both cases, increased internal connectivity potentially leads to a percolated, physically bonded network (electrostatic or hydrogen bonds) at sufficient loadings.

A major focus of clay–polymer nanocomposite research has been on efficient intercalation and exfoliation of the clay within a polymer matrix. Exfoliation tends to be most desirable in order to maximize the effect of the clay at a given clay volume fraction.⁴ The natural hydrophilicity of clay makes exfoliation with hydrophobic polymers difficult to achieve. Intercalation/exfoliation requires the polymer and clay to have some affinity for each other to allow the polymer to diffuse in between the clay sheets. Approaches to introduce favorable interactions rely

Received: March 26, 2019

Revised: June 29, 2019

on compatibilizers, typically a polar oligomer,¹² or copolymers with polar and nonpolar repeat units as the polymer matrix,¹³ with the latter approach being used in this study.

Sun and co-workers demonstrated the exfoliation of organically modified montmorillonite (oMMT) clay with low molecular weight, telechelic polybutadiene (tPB), end-functionalized with either hydroxyl or carboxyl terminal groups.^{14,15} Exfoliation was achieved by annealing at elevated temperatures without any other external energy input (no shearing, no sonication). This “self-exfoliation” of oMMT was found to occur even when diluting the number density of functional groups in the PB matrix by blending tPB with nonfunctionalized PBs.^{16,17} Explanations of the self-exfoliation mechanism remain rather speculative. However, for all of the above experiments, tPB functional groups were found to be essential to achieve clay exfoliation.

To date, self-exfoliation in PB has only been achieved with tPB of fairly low viscosity. Because of lack of variation of the polymer matrix, the significance of end-functionalization of the PB and/or the need for mobility of the PB matrix remains unclear. One method to achieve this is through post-polymerization modification in which polar functional groups can be incorporated to create random copolymers, with thiol–ene click chemistry being one of most commonly used techniques.¹⁸ David and Kornfield used thiol–ene click chemistry to graft various heterofunctional thiol molecules to the backbone of PB.¹⁹ With appropriate functional groups incorporated into the copolymer, the polymer can interact favorably with a given nanoparticle. However, the variation of functional groups may alter the polymer’s physical properties (before even adding any particles). This is important since the incorporation of hydrogen bonding groups onto the polymer’s backbone has been demonstrated to have major consequences on the polymer’s linear viscoelastic (LV) properties.^{20–22} For example, Stadler and de Lucca Freitas grafted urazole groups to a PB matrix and observed increased connectivity and longer relaxation times as the number of hydrogen bonding groups increased. This stems from the increased polymer–polymer interactions and is also reflected in the changes of other physical properties, such as the glass transition temperature.^{20,22}

Selecting thiol–ene click chemistry for synthesizing randomly functionalized polybutadiene (rPB) allowed us to systematically vary the hydroxyl group concentration and learn about its role in the self-exfoliation process. Additional hydroxyl groups attached to the PB backbone intensify polymer–polymer interactions and consequently reduce the molecular mobility. A detailed analysis was performed to separate the polymer–polymer from polymer–clay interactions. These experiments suggest that self-exfoliation is governed by both appropriate functionalities, even if it is random, and by sufficient polymer mobility. Without enough mobility, only limited exfoliation could be achieved.

EXPERIMENTAL SECTION

Materials. PB was functionalized by grafting mercaptoethanol to the polymer backbone. Two types of PB, low (24% 1,2 addition) and high vinyl (84% 1,2 addition) PB, with reported M_n values of 5000 and 2150 g/mol, respectively, were purchased (Sigma). Hydroxy-4-(2-hydroxyethoxy)-2-methylpropiophenone was used as the photoinitiator (Sigma). The solvent was tetrahydrofuran (THF) (Fisher Scientific). oMMT clay particles were obtained from Fenghong Clay Corporation with an octadecyltrimethyl ammonium cation with an initial spacing of 2.1 nm. A small amount of antioxidant (Irganox

B225 from BASF) (0.2 wt %) was added to the composite mixtures to prevent degradation.

Grafting Procedure for rPB. The grafting of 2-mercaptoethanol to PB followed a standardized procedure. First, 2 g of PB, 10 wt % photoinitiator, and desired amounts of 2-mercaptoethanol were dissolved into 10 mL of THF. The solution was purged with nitrogen for 15 min and exposed to 365 nm ultraviolet light for 3 h. The resulting polymer was precipitated into deionized water and dried under vacuum at 65 °C for 2 days to remove the residual solvent. The molar ratio of the polymer with respect to 2-mercaptoethanol varied between 0 and 5.2 mM (Table 1). Grafting to the low vinyl PB

Table 1. Concentrations of 2-Mercaptoethanol and PB To Generate the Polymer Series Along with Tabulated Values from ¹H NMR, GPC (Based on PS Standard), and DSC with High Vinyl (84% 1,2 Addition) PB

thiol input (mm)	PB vinyl input (mm)	% vinyl converted (v)	M_n (g/mol)	dispersity	$T_{g,DSC}$ (°C)	$T_{g,rheo}$ (°C)	$T_{g,rheo} - T_{g,DSC}$
0	0	0	5000	1.57	−25		
0.57	74	1.6	5100	1.81	−22	−19	3
2.56	74	3.0	5500	1.71	−14	−11	3
3.42	74	6.2	5900	1.81	−9	−5	4
4.28	74	7.1	5900	1.81	−6	−2	4
5.13	74	7.9	6100	2.01	−2	4	6

needed to be performed at a reduced photoinitiator concentration of 0.6 wt % (with respect to polymer) and a higher THF solvent volume of 250 mL to avoid interchain cross-linking.

Composite Preparation. Special precautions were taken when fabricating the composite since the intercalated/exfoliated PB/clay nanocomposite is known to irreversibly soften under strain.²³ Inappropriate sample loading into the rheometer would alter the sample’s structure and rheological properties. To avoid this loss of internal connectivity, it is essential to load the gently mixed sample in the rheometer before any significant intercalation/exfoliation occurs, recognizing the fact that structure development in a freshly mixed rPB/clay sample requires time. Suspensions of oMMT (8 wt %) in rPB and 0.2 wt % antioxidant were gently hand-mixed to homogenize. Then, the samples were immediately loaded into the rheometer. Annealing at 80 °C for 10 h in the rheometer finalized the nanocomposite structure, ready for small amplitude oscillatory shear (SAOS) characterization. An additional 2 h anneal and a second SAOS characterization were also performed. For all composites tested, the two SAOS master curves were found to be identical, indicating that a steady-state had been established after the first anneal. This is to say, no further structure development occurred during the second annealing under quiescent conditions.

Chemical Characterization. The molecular weight of the rPB was characterized with a THF gel permeation chromatography (GPC) instrument (Agilent 1260 Infinity) equipped with a refractive index detector. Molecular weight and dispersity were determined using polymethylmethacrylate standards. The grafting density of the rPB samples was measured via ¹H nuclear magnetic resonance (NMR) spectroscopy (Bruker AVANCE III HD 500 MHz NMR).

Differential Scanning Calorimetry. The rPB glass transition temperature (T_g) was measured using differential scanning calorimetry (DSC) with a TA Instrument Q200 calorimeter with nitrogen gas purge flow at 5 mL/min between −70 and +40 °C at a heating rate of 10 K/min.

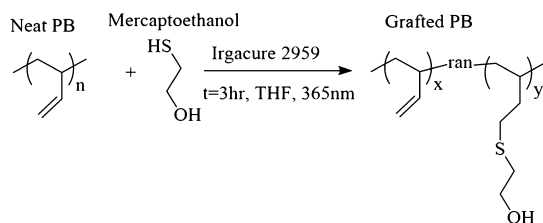
Rheology. A stress-controlled Malvern Kinexus Pro+ rheometer with a 20 mm parallel plate fixture was used for LV measurements. SAOS frequency sweeps were repeated from $\omega = 1$ –100 rad/s at a strain amplitude of 0.1% between 0 and 80 °C in 10 K steps. The rheological data were analyzed and plotted with the IRIS Rheo-Hub software.

X-ray Scattering. Medium-angle X-ray scattering (MAXS) in a Ganesha 300 XL SAXS instrument characterized the spacing between clay sheets. Samples were exposed to the X-ray source for 180 s at a wavelength of 0.154 nm. The sample to detector distance was set to a fixed distance of 0.691 m with a 2 mm beam stop. Similar experiments have been reported to distinguish intercalation from exfoliation in clay nanocomposites.^{14,15,17}

RESULTS

Grafting of Hydroxyl Groups. The double bonds of the high vinyl PB (84%, 1,2-addition) were reacted with 2-mercaptoethanol using thiol–ene click chemistry. The synthetic scheme for grafting is shown in Scheme 1. By

Scheme 1. Synthesis of Grafted PB with 2-Mercaptoethanol



varying the concentration of 2-mercaptoethanol in the reaction, different degrees of grafting were achieved. ¹H NMR measurements quantified the average degree of grafting, which was calculated by taking the ratio of the protons alpha to the grafted hydroxyl groups relative to the remaining unreacted double bonds, Table 1 (¹H NMR spectra in Supporting Information Figure S1). The average degree of grafting ranged from 0 to 7.9 mol % when 2-mercaptoethanol was increased from 0 to 5.13 mM in the reaction mixture. It should be noted that the grafting reaction is random; some chains remain without grafts, whereas others have higher grafting than the reported average grafting. The molecular weight and dispersity are summarized in Table 1 from GPC, and the traces for each sample are shown in the Supporting Information (Figure S2). As expected, increasing the initial concentration of 2-mercaptoethanol increased both the degree of grafting and the molecular weight. Less expected was the increase in the dispersity of the molecular weight. Potential reasons for this will be addressed in the Discussion section.

Characterization of Polymer Melt. DSC was used to tabulate the glass transition temperatures (T_g) of the hydroxyl-grafted PB series. It was found that the hydroxyl grafting caused PB's T_g to increase (Table 1). At the highest level of grafting in this study (7.9% mol grafting), T_g increased by approximately 25 K. The increase in T_g is attributed to increased interchain interactions which reduces polymer mobility.

SAOS experiments on the rPB samples can be merged into the master curves of Figure 1 by time–temperature superposition to a common reference temperature. Storage modulus (Figure 1a), loss modulus (Figure 1b), and complex viscosity (Figure 1c) all increased with greater hydroxyl content. This again may be attributed to additional connectivity due to increased polymer–polymer interactions. Each of the rPB still exhibits traditional terminal liquid behavior ($G' \approx \omega^2$, $G'' \approx \omega^1$, and a constant complex viscosity at low frequencies). Relaxation times were found to get longer with hydroxyl grafting, which is shown in Supporting Information (Figure S3) along with the shift factors belonging to the SAOS master curves. The time–temperature shifting follows WLF scaling. All of the polymers' LV properties appeared to be similar, exhibiting comparable shapes of their dynamic moduli.

For a constant reference temperature ($T_{ref} = 20\text{ }^\circ\text{C}$), the relative distance to T_g decreases as grafting increases. Alternatively, rheological data are best compared at a constant distance ΔT above their respective T_g . To normalize T_g effects, we chose a varying reference temperature $T_{ref} = T_{g,DSC} + \Delta T$, where ΔT was kept constant at 45 K and $T_{g,DSC}$ was varied according to DSC measurements on each of the rPBs. This collapsed all SAOS data onto a single master curve, but the superposition was not completely satisfactory. To improve the superposition, each polymer's reference temperature was slightly adjusted. Doing so resulted in a single curve where the neat PB could be used as the reference (Figure 2a,b). On the basis of this optimized superposition of the LV data, a new (“rheological”) glass transition temperature was found, $T_{g,rheo}$, with the reference temperature, $T_{ref} = T_{g,rheo} + \Delta T$, as determined by LV data shifting. A remarkable agreement was found between the T_g from the two different characterization methods (Figure 2, Table 1).

Separation of Grafting from Hydrogen-Bonding Effects on T_g . With grafting, T_g increased drastically (see Table 1), but it was unclear whether this increase was due to grafting or it was caused specifically by the hydroxyl functionality. To answer this, mercaptobutane, containing no hydroxyl groups, was grafted to the PB matrix at 4.2% grafting density using the same synthetic procedure. Figure 3 compares the LV properties of the mercaptobutane-grafted PB control sample with the neat PB (Figure 3). Both polymers had similar LV properties and the same T_g ($-25\text{ }^\circ\text{C}$) through DSC. This suggests that the observed increases in T_g are because of the addition of hydrogen bonding of the hydroxyl groups, not the grafting itself.

Addition of Clay to the Modified Polymer. Sample preparation required specific precautions, as described above. Immediately after adding 8 wt % clay into the functionalized polymers, the samples were placed in between the rheometer

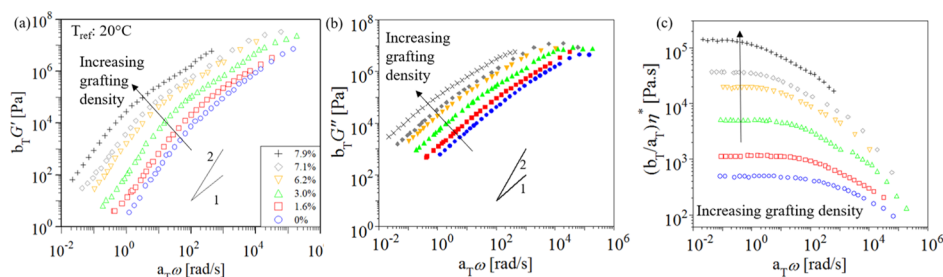


Figure 1. Storage modulus (a), loss modulus (b), and complex viscosity (c) as a function of frequency at various hydroxyl grafting densities.

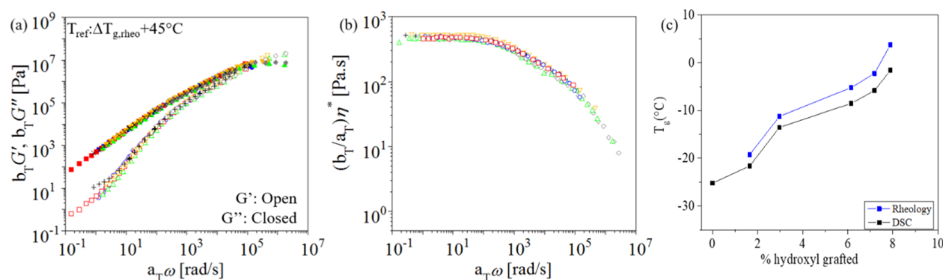


Figure 2. Collapsed SAOS master curves when shifting the reference for the storage and loss modulus (a) and complex viscosity (b). $T_{g,rheo}$ and T_g from DSC are plotted as a function of the grafting density (c).

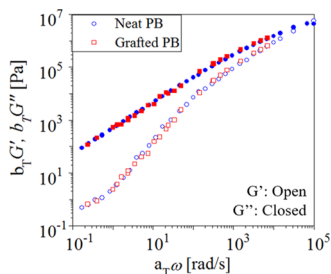


Figure 3. SAOS master curves of neat PB and 4.2 mol % PB grafted with mercaptobutane. The T_g and LV response of the mercaptobutane-grafted PB matched that of the neat PB.

fixtures and annealed for 10 h at 80 °C. Once the structure stabilized, SAOS measurements were performed for a wide range of temperatures and frequencies. The data was superimposed into master curves at a reference temperature of $T_{g,rheo} + 45$ K. The composites' storage modulus and $\tan \delta$ (Figure 4a), the loss modulus (Figure 4b), and Winter plot (Figure 4c) at various hydroxyl grafting densities are shown in Figure 4. All composites are physical gels marked by a low-frequency plateau in the storage modulus and a downturn in $\tan \delta$. The Winter plot provides complimentary evidence of the solid structure marked by the straight vertical line observed in the low-modulus/low-frequency regime.^{24–26} The formation only occurred when hydroxyl groups were grafted to the polymer matrix (Figure S4).

Surprisingly, samples with the highest and the second highest degrees of grafting (crosses and diamonds, respectively) exhibited the lowest and second lowest connectivity, respectively, that is, the lowest moduli in the low-frequency regime. To quantify the decrease in the cross-linking density, a second free shift was used. Specifically, concentration–time free shifting was able to superimpose all curves in Figure 4 onto a single curve. The vertical shift expressed the change in modulus by setting the 1.6% grafted sample as the reference. In

addition, the corresponding change in relaxation times was calculated from the horizontal shift for each composite. At low and intermediate degrees of grafting, the modulus in the low-frequency regime was higher and appeared to be independent of the grafting density. Therefore, for this set of grafted PB with a high vinyl content (84% 1,2 addition), an intermediate range of hydroxyl grafting exists at which the internal connectivity maximizes. As further hydroxyl grafting was incorporated, the overall modulus began to decrease, and characteristic relaxation times got longer (Figure 5a). We

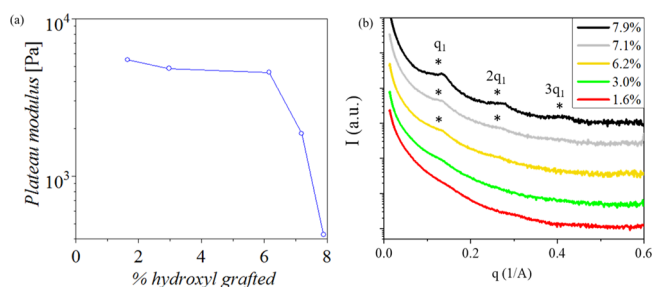


Figure 5. Composite's normalized plateau modulus and characteristic relaxation time at various grafting densities (a). X-ray scattering profiles of composites at various hydroxyl grafting densities after structure formation in the rheometer. Highly grafted composites have a lower extent of exfoliation marked by the appearance of a peak (even higher order peaks). All samples contained 8 wt % clay.

attribute the decrease in connectivity to decreased exfoliation. This could either be due to the concentration of hydroxyl groups or reduced molecular mobility of rPBs associated with their high T_g . In this study, the plateau modulus was defined by extrapolating the low-frequency regime of the storage modulus shown in Figure 4a.

X-ray scattering was used to determine the degree of exfoliation of the clay in all composites (Figure 5). MAXS

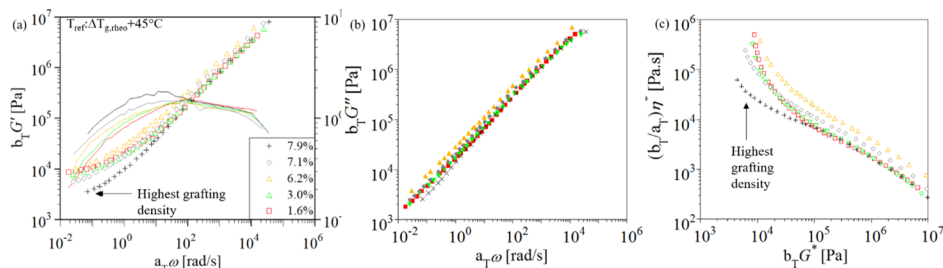


Figure 4. LV response of the rPB/clay nanocomposites expressed as the storage modulus and $\tan \delta$ (a), loss modulus (b), and Winter plot (c). A decrease in connectivity is seen at high hydroxyl grafting. Composites were prepared with 8 wt % clay.

showed no scattering features corresponding to ordered clay sheets for the rPB/clay nanocomposites with low grafting densities. This indicates that exfoliation was achieved only at low grafting densities. At high grafting densities, a first order peak appears, and eventually higher order peaks at higher grafting density appear. These are associated with the spacing of intercalated clay sheets (4.8 nm).

Separating Mobility and Functional Group Concentration. PB of high vinyl content (84% 1,2 addition; $T_g = 25$ °C) provided the starting polymer backbone for grafting the hydroxyl groups. There is a possibility that the exfoliation dynamics of clay/rPB could be dominated by either lack of mobility due to its close proximity to its T_g or having too many hydroxyl functionalities. To decouple these two phenomena, the above experiments were paralleled with a highly grafted, low vinyl PB, which is known to have a much lower T_g . The new starting material was PB of 24% 1,2 addition. It is well established that decreasing the vinyl content in PB lowers the T_g and thus increases the molecular mobility.²² Because of the temperature limitations of DSC, T_g for the 24% 1,2 addition PB could not be directly determined; however, previous reports have assigned a PB of similar composition with a T_g at approximately -90 °C.²⁴ With this low T_g PB, mercaptoethanol was grafted onto the polymer backbone at 9.1 mol %. The complex viscosity of the neat and grafted polymers at 20 °C is compared in Figure 6a. The viscosity of the low vinyl, highly

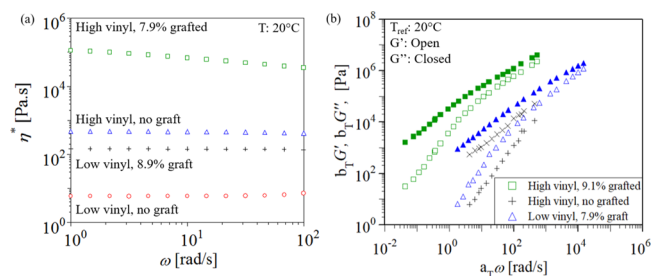


Figure 6. Complex viscosity (a) and SAOS master curves (b) of the high vinyl, 7.9% grafted (gray), high vinyl, no grafting (blue), and low vinyl, 9.1% grafted and low vinyl, no grafting (green) PB samples.

grafted rPB is even lower than that of the high vinyl, neat PB (no grafts). Thus, the low vinyl, grafted PB is in fact highly mobile even at higher degrees of grafting. The corresponding SAOS master curves of the two grafted polymers are shown in Figure 6b.

Clay (8 wt %) was added to the low vinyl rPB to again create stress-free nanocomposites and test them in the rheometer.

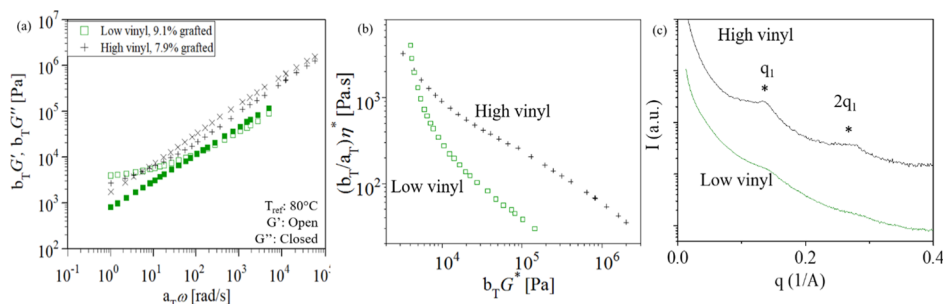


Figure 7. Dynamic modulus (a), Winter plot (b), and MAXS scattering profiles (c) of the highly grafted nanocomposites with different vinyl contents. Composites were prepared with 8 wt % clay.

The dynamic moduli, Winter plot, and MAXS scattering profile of the two grafted clay–polymer nanocomposites are compared in Figure 7a–c, respectively. The nanocomposite of low vinyl rPB has a significantly lower modulus in the high-frequency regime and spans over a smaller frequency range at low experimental temperatures. The glassy region is outside the experimental range of the low vinyl PB composites. In the low-frequency regime, the low vinyl composite's storage modulus is greater, specifically the plateau modulus. This is particularly evident in the low modulus portion of the Winter plot (Figure 7b). This corresponds to higher connectivity and, in this case, a higher physical cross-linking density. When comparing the MAXS scattering profiles, the low vinyl polymer nanocomposite reached a higher degree of exfoliation, correlating nicely with the rheology data.

DISCUSSION

Telechelic polymers with their functional ends have drawn extensive attention.^{27–29} Such linear polymers with functional end-groups are envisioned to assemble into loops on particle surfaces and/or bridges between two particles. This is interesting in the context of this study since the PB matrix in the original exfoliation work of Sun was telechelic.¹⁴ However, the significance of having the polymer telechelic had not been explored. As shown by the randomly grafted PB series (rPB), while functional groups are required to induce self-exfoliation, these functional groups can be placed anywhere along the PB backbone. Exfoliation was achieved at hydroxyl functionalities as low as 1.6 mol %, which corresponds to approximately one hydroxyl group per chain, on average. The ability to exfoliate the clay at such a low concentration of functional groups agrees with the findings of Wang and co-workers who showed that a blend of nonfunctionalized and rPB was sufficient for achieving exfoliation.¹⁶ It also appears that the composites' LV properties at low-to-intermediate grafting densities are independent of hydroxyl grafting. At higher grafting densities, there was a decrease in connectivity along with a transition from clay exfoliation to intercalation. This provides some insight into the self-exfoliation process and the origin of connectivity, which will be addressed later in this section.

In addition to random placement of the hydroxyl functional group, a consequence of the hydroxyl grafting was that the polymer's molar mass increased, as expected,¹⁹ along with the dispersity. The grafting of mercaptoethanol more than doubles the molecular weight of a backbone repeat unit. However, the grafting of mercaptoethanol does not fully account for the 20% increase in the molecular weight observed. Additional side reactions may have occurred with the most likely being

interchain cross-linking between the double bonds in the polymer's backbone.¹⁶ This assumption is supported by the asymmetric broadening in the GPC traces of the grafted polymers. This indicates that some individual chains increase in molecular weight, presumably due to chain coupling, which would account for both the molecular weight and dispersity increases. There appears to be no correlation between the broadening of the GPC peak (related to dispersity) and the grafting density. Since all polymers remained soluble and exhibited terminal flow behavior over the entire frequency range tested, any side reactions and dispersity increase that may have occurred are considered negligible.

Hydroxyl grafting increased the T_g of the synthesized rPBs (Table 1). The increase in T_g stems from the additional interchain interactions from the hydrogen bonding between the grafted hydroxyl groups. These interactions provide additional polymer–polymer connectivity and decrease chain mobility which was captured with the master curves. A similar rheological response has been reported for several other hydrogen-bonding systems.^{20–22} To account for the decrease in mobility, rPBs were referenced uniformly by keeping the same distance away from T_g ($T_g + 45$ K). This was an effective method to account for differences in T_g and resulted in the rPBs' LV curves superimposing onto a single curve. Establishing this analysis was critical when adding clay to these polymers. A similar approach for how to account for T_g has been applied to polystyrene/polystyrene oligomer blends.

A key aspect of this work was to understand the connectivity clay provided to the rPB matrix, independent of T_g . Therefore, the reference temperatures of SAOS master curves were set at a fixed distance above T_g with an attempt to equally emphasize the LV contributions of T_g . The validity of this approach is verified by the high-frequency response of the composites. In this regime, the SAOS master curves converge as they dynamically approach the glassy state since they are all an equal distant away from T_g . Even much above T_g , the overall connectivity in the material dominates the low-frequency behavior. The material is a physical gel with a plateau modulus that directly correlates with the (physical) cross-linking density of the gel. At low-to-intermediate grafting densities, the overall connectivity was almost constant and showed successful clay exfoliation. This suggests that the location of the hydroxyl groups (end-terminated vs grafted) is not critical for exfoliation.

For the highly functionalized rPB, exfoliation appeared to be limited. The decreased exfoliation is believed to be caused by the reduced mobility, not the concentration of the functional groups. In the initial series, this was impossible to decouple since the addition of hydroxyl groups decreased the mobility. To verify this, highly grafted (9.1%) rPB was synthesized again using a low vinyl PB with a lower T_g (~ -90 °C). Because of the polymer's low T_g , it can be considered mobile relative to the previous series. This highly grafted, highly mobile rPB successfully exfoliated the clay as shown by the lack of peaks in the SAXS profile. Its composite reached a high level of internal connectivity. This clearly supports the claim that clay exfoliation is mobility limited and not restricted to a low concentration of functional groups.

CONCLUSIONS

In this study, key matrix criteria were established for the self-exfoliation of clay in PB. These findings can be applied to a variety of other 2D nanoparticle/polymer composites.

Specifically, the role of functionalization and polymer mobility have been elucidated. The functionalization of the PB matrix is necessary for sufficient interactions between the clay and the polymer, but the number and location of functional groups are not critical. Even at a low hydroxyl density (as low as 1 hydroxyl group per chain), exfoliation can still occur. With additional grafting of hydroxyl groups, PB's T_g increases and thus lowers the mobility of the matrix. Experiments with highly functionalized PB of varying mobilities show that the extent of exfoliation can be drastically limited by mobility, presumably by slowing the polymer's ability to diffuse between the clay sheets. On this basis, we propose a new mechanism to understand the clay exfoliation in which intercalation occurs only if there are sufficient polymer–clay interactions, but beyond intercalation, exfoliation is facilitated by polymer mobility. These findings present key parameters when considering low-energy methods for exfoliation of 2D layered materials in polymer matrices.

ASSOCIATED CONTENT

Supporting Information

The Supporting Information is available free of charge on the ACS Publications website at DOI: 10.1021/acs.macromol.9b00616.

Proton NMR used to quantify the grafting density, THF GPC traces of the reacted PBs, shift factors and WLF fit of the grafted polymers and the characterization relaxation of the grafted polymers, and master curves of neat PB with and without clay (PDF)

AUTHOR INFORMATION

Corresponding Author

*E-mail: winter@umass.edu. Phone: 413-545-0922.

ORCID

E. Bryan Coughlin: 0000-0001-7065-4366

H. Henning Winter: 0000-0002-5470-7736

Notes

The authors declare no competing financial interest.

ACKNOWLEDGMENTS

We would like to acknowledge the American Chemical Society Petroleum Research Fund (grant number 58675-ND10) for supporting this work.

REFERENCES

- (1) Kim, W.-g.; Nair, S. Membranes from Nanoporous 1D and 2D Materials: A Review of Opportunities, Developments, and Challenges. *Chem. Eng. Sci.* **2013**, *104*, 908–924.
- (2) Krishnamoorti, R.; Giannelis, E. P. Rheology of End-tethered Polymer Layered Silicate Nanocomposites. *Macromolecules* **1997**, *30*, 4097–4102.
- (3) Splendiani, A.; Sun, L.; Zhang, Y.; Li, T.; Kim, J.; Chim, C.-Y.; Galli, G.; Wang, F. Emerging Photoluminescence in Monolayer MoS₂. *Nano Lett.* **2010**, *10*, 1271–1275.
- (4) Sinha, R. S.; Okamoto, M. Polymer/Layered Silicate Nanocomposites: A Review from Preparation to Processing. *Prog. Polym. Sci.* **2003**, *28*, 1539–1641.
- (5) Kojima, Y.; Usuki, A.; Kawasumi, M.; Okada, A.; Fukushima, Y.; Kurauchi, T.; Kamigaito, O. Mechanical Properties of Nylon 6-Clay Hybrid. *J. Mater. Res.* **1993**, *8*, 1185–1189.
- (6) Lee, K. M.; Han, C. D. Effect of Hydrogen Bonding on the Rheology of Polycarbonate/Organoclay Nanocomposites. *Polymer* **2003**, *44*, 4573–4588.

- (7) Tien, Y. I.; Wei, K. H. Hydrogen Bonding and Mechanical Properties in Segmented Montmorillonite/Polyurethane Nanocomposites of Different Hard Segment Ratios. *Polymer* **2001**, *42*, 3213–3221.
- (8) Okamoto, M.; Nam, P. H.; Maiti, P.; Kotaka, T.; Hasegawa, N.; Usuki, A. A House of Cards Structure in Polypropylene/Clay Nanocomposites under Elongational Flow. *Nano Lett.* **2001**, *1*, 295–298.
- (9) Lagaly, G.; Ziesmer, S. Colloid Chemistry of Clay Minerals: The Coagulation of Montmorillonite Dispersions. *Adv. Colloid Interface Sci.* **2003**, *100–102*, 105–128.
- (10) Tombácz, E.; Szekeres, M. Colloidal behavior of aqueous montmorillonite suspensions: the specific role of pH in the presence of indifferent electrolytes. *Appl. Clay Sci.* **2004**, *27*, 75–94.
- (11) Tombácz, E.; Szekeres, M. Surface Charge Heterogeneity of Kaolinite in Aqueous Suspension in Comparison with Montmorillonite. *Appl. Clay Sci.* **2006**, *34*, 105–124.
- (12) Kawasumi, M.; Hasegawa, N.; Kato, M.; Usuki, A.; Okada, A. Preparation and Mechanical Properties of Polypropylene–Clay Hybrids. *Macromolecules* **1997**, *30*, 6333–6338.
- (13) Wang, K. H.; Choi, M. H.; Koo, C. M.; Choi, Y. S.; Chung, I. J. Synthesis and Characterization of Maleated Polyethylene/Clay Nanocomposites. *Polymer* **2001**, *42*, 9819–9826.
- (14) Sun, P.; Zhu, J.; Chen, T.; Yuan, Z.; Li, B.; Jin, Q.; Ding, D.; Shi, A. Rubber/exfoliated-clay nano-composite gel: Direct exfoliation of montmorillonite by telechelic liquid rubber. *Chin. Sci. Bull.* **2004**, *49*, 1664–1666.
- (15) Chen, T.; Zhu, J.; Li, B.; Guo, S.; Yuan, Z.; Sun, P.; Ding, D.; Shi, A.-C. Exfoliation of Organo-Clay in Telechelic Liquid Polybutadiene Rubber. *Macromolecules* **2005**, *38*, 4030–4033.
- (16) Wang, X.; Tao, F.; Xue, G.; Zhu, J.; Chen, T.; Sun, P.; Winter, H. H.; Shi, A. C. Enhanced Exfoliation of Organoclay in Partially End-Functionalized Non-Polar Polymer. *Macromol. Mater. Eng.* **2009**, *294*, 190–195.
- (17) Tanna, V. A.; Zhou, Y.; Henning Winter, H. Effect of Platelet Size in a Soft Nanocomposite: Physical Gelation and Yielding. *J. Rheol.* **2018**, *62*, 791–800.
- (18) Hoyle, C. E.; Bowman, C. N. Thiol-ene Click Chemistry. *Angew. Chem., Int. Ed.* **2010**, *49*, 1540–1573.
- (19) David, R. L. A.; Kornfield, J. A. Facile, Efficient Routes to Diverse Protected Thiols and to Their Deprotection and Addition to Create Functional Polymers by Thiol–Ene Coupling. *Macromolecules* **2008**, *41*, 1151–1161.
- (20) de Lucca Freitas, L. L.; Stadler, R. Thermoplastic Elastomers by Hydrogen Bonding. 3. Interrelations between Molecular Parameters and Rheological Properties. *Macromolecules* **1987**, *20*, 2478–2485.
- (21) Müller, M.; Seidel, U.; Stadler, R. Influence of Hydrogen Bonding on the Viscoelastic Properties of Thermoreversible Networks: Analysis of the Local Complex Dynamics. *Polymer* **1995**, *36*, 3143–3150.
- (22) Lewis, C. L.; Stewart, K.; Anthamatten, M. The Influence of Hydrogen Bonding Side-Groups on Viscoelastic Behavior of Linear and Network Polymers. *Macromolecules* **2014**, *47*, 729–740.
- (23) Tanna, V.; Wetzels, C.; Henning Winter, H. Onset of Nonlinearity and Yield Strain of a Model Soft Solid. *Rheol. Acta* **2017**, *56*, 527–537.
- (24) Winter, H. H. Three Views of Viscoelasticity for Cox-Merz Materials. *Rheol. Acta* **2009**, *48*, 241–243.
- (25) Vinogradov, G. V.; Malkin, A. Y.; Kulichikhin, V. G. Microstructure and rheological properties of polybutadienes. *J. Polym. Sci., Part A-2* **1970**, *8*, 333–353.
- (26) Carella, J. M.; Graessley, W. W.; Fetters, L. J. Effects of Chain Microstructure on the Viscoelastic Properties of Linear Polymer Melts: Polybutadienes and Hydrogenated Polybutadienes. *Macromolecules* **1984**, *17*, 2775–2786.
- (27) Ginzburg, V. V.; Balazs, A. C. Calculating Phase Diagrams for Nanocomposites: The Effect of Adding End-Functionalized Chains to Polymer/Clay Mixtures. *Adv. Mater.* **2000**, *12*, 1805–1809.
- (28) Sinsawat, A.; Anderson, K. L.; Vaia, R. A.; Farmer, B. L. Influence of polymer matrix composition and architecture on polymer nanocomposite formation: Coarse-grained molecular dynamics simulation. *J. Polym. Sci., Part B: Polym. Phys.* **2003**, *41*, 3272–3284.
- (29) Malvaldi, M.; Allegra, G.; Ciardelli, F.; Raos, G. Structure of an Associating Polymer Melt in a Narrow Slit by Molecular Dynamics Simulation. *J. Phys. Chem. B* **2005**, *109*, 18117–18126.
- (30) Wagner, M. H. Scaling Relations for Elongational Flow of Polystyrene Melts and Concentrated Solutions of Polystyrene in Oligomeric Styrene. *Rheol. Acta* **2014**, *53*, 765–777.